

Giant anisotropic magnetoresistance at low magnetic fields in a layered semiconductor

H. Murakawa,^{1,*} Y. Nakaoka,¹ T. Kida,² M. Hagiwara,² H. Sakai,¹ and N. Hanasaki¹¹Department of Physics, Osaka University, Toyonaka, Osaka 560-0043, Japan²Center for Advanced High Magnetic Field Science (AHMF), Graduate School of Science, Osaka University, Toyonaka, Osaka 560-0043, Japan

(Received 11 February 2022; accepted 12 May 2022; published 31 May 2022)

Materials exhibiting a drastic change in electrical resistivity depending on magnetic-field direction is of great interest and is rarely seen in real systems. We report the huge anisotropic magnetoresistance ratio exceeding 7500 at low-magnetic field of 0.4 T at 2 K in the layered magnetic semiconductor $\text{CeTe}_{1.83}\text{Sb}_{0.17}$ with extremely low carrier density in charge-density-wave state. We found that the electrical resistivity is governed only by the out-of-plane component of magnetization and steeply decreases nearly four orders of magnitude in the magnetic field along the c axis. In contrast, it is quite insensitive to the in-plane component of magnetization and huge anisotropy is preserved even in a much higher magnetic field.

DOI: [10.1103/PhysRevMaterials.6.054604](https://doi.org/10.1103/PhysRevMaterials.6.054604)

I. INTRODUCTION

Magnetoresistance, i.e., change of electrical resistivity in a magnetic field, is one of the most fundamental phenomena in materials [1,2]. The most common example is the transition-metal-based magnetic multilayer system [3] that exhibits the large magnetoresistance in a very low magnetic field and is used in various memory and sensing devices. Besides the practical interest in room-temperature operation, the phenomenon itself is very exciting especially at lower temperatures where the essential role of magnetic interaction for charge carrier mobility becomes clear in the absence of thermal fluctuation and, in some cases, the size of magnetoresistance becomes enormous. Semimetal is known to show huge magnetoresistance ratio that increases monotonically up to several orders of magnitude in a high magnetic field due to the cancellation of Hall voltage by electrical charge compensation [4,5]. By improving the crystal quality to achieve the ultrahigh carrier mobility and perfect electrical charge compensation, the magnetoresistance ratio in semimetal is much enhanced up to several million [6,7]. The perovskite manganite oxides family is the strongly correlated electron system that exhibits the giant negative magnetoresistance [8,9]. The electrical resistivity in those hole-doped Mott insulators is highly dependent on the relative orientation of the local magnetic moment in neighboring sites since charge transfer gap is determined by the on-site Hund coupling between itinerant spin and local magnetic moment. Similarly, the large negative magnetoresistance occurs in the magnetic molecular conductors by the intramolecular interaction between itinerant π electron spin and localized magnetic moment [10–12]. In addition, huge size of negative magnetoresistance is seen in the rare-earth compounds with relatively lower carrier density by magnetic polaron mechanism [13]. The electrical resistivity in these materials decreases dramatically by several

orders of magnitude by applying a magnetic field of several tesla, accompanied by the transition from antiferromagnetic to forced-ferromagnetic order [14–16]. Besides the large response in electrical resistivity to the magnetic-field amplitude, the sensitivity to a magnetic-field direction is another useful property. However, in most of the known magnetic conductors including the above systems, the anisotropy of magnetoresistance is limited in the scale of the magnetic anisotropy and is generally much smaller than the value of magnetoresistance itself, since reduction of the electrical resistivity occurs in the magnetization increasing process, irrespective of the magnetic-field direction. Thus large anisotropic magnetoresistance is rarely seen especially in low magnetic-field range.

Among various magnetic conductors, the layered low carrier density system shows unique magnetoresistance that is not classified in the above mentioned common mechanism for antiferromagnetic conductors. CeTe_2 is the quasi-two-dimensional low carrier density material [17–20], the structure of which is formed by the alternating stacking of the magnetic insulating [CeTe(1)] layer and the semiconducting Te(2) layer [Fig. 1(a)]. At room temperature, it has the tetragonal symmetry and belongs to the space group 129: ($P4/nmm$). Owing to the good nesting of the sheetlike Fermi surfaces formed by $\text{Te-}5p_x$ and $5p_y$ orbitals in the Te(2) square network, the charge-density-wave state is realized above room temperature and a narrow gap opens in an almost entire area of the Fermi surfaces, resulting in the low carrier density [21–23]. Powder neutron diffraction measurements indicate that short-range ferromagnetic order develops below 10 K, where a magnetic moment of Ce in the ab plane aligns along the c axis ([001]). With further decreasing temperature, these ferromagnetic layers stack antiferromagnetically and the prospect of the ferrimagnetic long-range order was discussed [24,25]. This characteristic magnetic state influences the electrical conductivity in the spatially separated layers and, at low temperatures, negative magnetoresistance was observed [17,18]. However, the size of magnetoresistance was only less than 30%, and the temperature and magnetic field dependence

*murakawa@phys.sci.osaka-u.ac.jp

of electrical resistivity was not simple due to parallel conduction of the other charge carrier pocket irrelevant to the charge-density-wave state that hinders the essential magneto-transport phenomena in this system [26]. Thus the role of the local magnetic correlation for the electrical conduction in the layered charge-density-wave semiconductor is yet unknown.

Here, we report the highly anisotropic giant negative magnetoresistance in the layered magnetic semiconductor $\text{CeTe}_{1.83}\text{Sb}_{0.17}$. Partial substitution of Te with Sb shifts Fermi level and removes an extra charge carrier pocket by hole doping, and the intrinsic charge-density-wave semiconductor is realized [26]. In the magnetically ordered state, we found that the electrical resistivity drastically decreases in the increasing process of the out-of-plane component of magnetization, reaching nearly four orders of magnitude reduction in a low magnetic field of 0.4 T along [001]. In contrast, only the small change is observed in electrical resistivity in a magnetic field normal to [001], resulting in a huge anisotropic magnetoresistance ratio exceeding 7500. We found the relationship between electrical resistivity and the out-of-plane component of magnetization in the entire variation process, while it is almost independent of the in-plane component of magnetization. Such huge anisotropic coupling between electrical conduction and magnetization is the source for the present drastic angular magnetoresistance.

II. EXPERIMENT

Single crystals of $\text{CeTe}_{1.83}\text{Sb}_{0.17}$ were obtained by the chemical vapor transport technique with iodine as a transport agency. The transmission Laue method was used to determine the crystal structure. Composition ratio of each element was precisely determined by the inductively coupled plasma method and was consistent in two samples. Electrical resistivity was measured by four probe method with an excitation current of 20 nA in the high-resistivity range below 20 K and up to 100 μA at room temperature. The gold paste was used for putting the gold wire to the sample. The output impedance of the current source and input impedance of the voltage meter are much higher than the highest resistance value measured in the sample.

III. RESULTS AND DISCUSSION

Figure 1(b) shows the temperature dependence of the magnetic susceptibility in $H \parallel [001]$ and $[100]$. Steep increase below 10 K in $H \parallel [001]$ indicates the short-range ferromagnetic order in the magnetic layer and the sharp kink at 4.0 K is the onset of the long-range order of the antiferromagnetic correlation between the ferromagnetic layers. Figure 1(c) shows the temperature dependence of the in-plane and out-of-plane electrical resistivity (ρ_{xx} and ρ_{zz}). Owing to the quasi-two-dimensional character, ρ_{zz} is 20–100 times higher than ρ_{xx} in the entire temperature range. Both ρ_{xx} and ρ_{zz} increase with decreasing temperature and become 10^9 times higher at 2 K compared to the room-temperature value. The intrinsic semiconductor originating from the charge-density-wave gap is rare in bulk materials because of the difficulty of the perfect nesting of three-dimensional Fermi surfaces. Although the precise evaluation of the

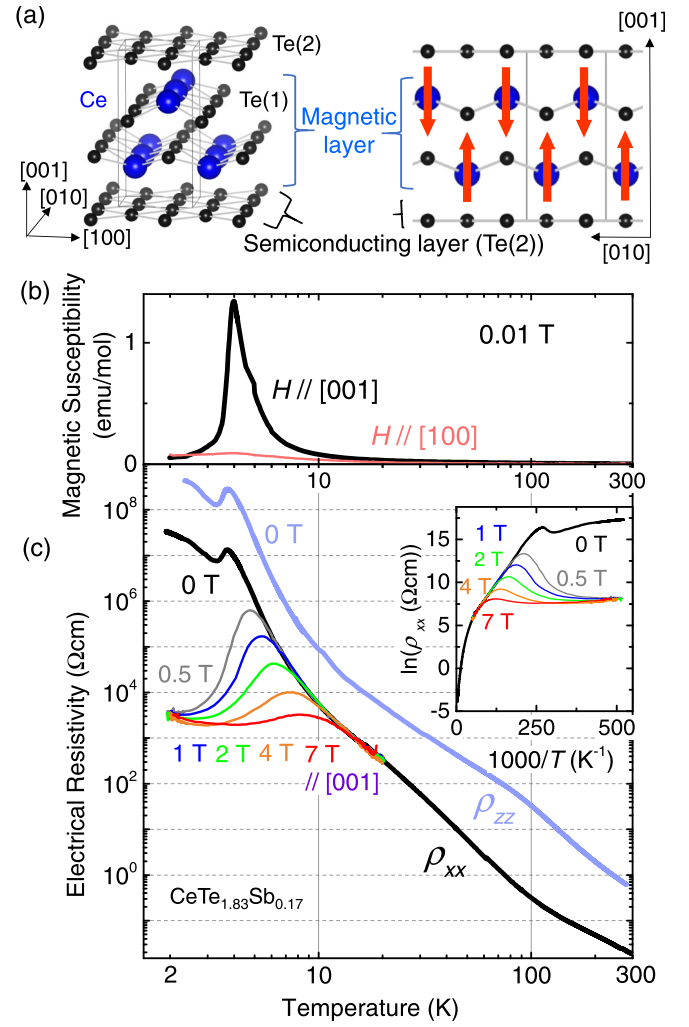


FIG. 1. (a) Crystal structure of $\text{CeTe}_{1.83}\text{Sb}_{0.17}$ and magnetic structure at the lowest temperature. (b), (c) Temperature dependence of (b) magnetization at 0.01 T in $H \parallel [001]$ and $[100]$ and (c) electrical resistivity in various magnetic fields along [001]. Inset shows the Arrhenius plot of ρ_{xx} .

total carrier density is difficult from the compensated Hall coefficient in our intrinsic semiconducting sample, it should be much lower than the previously reported metallic sample $\sim 10^{16} \text{ cm}^{-3}$ [27]. From the slope of the Arrhenius plot shown in the inset in Fig. 1(c), the excitation gap size at 0 T is determined to be 0.03 eV at around room temperature. Below 20 K, the slope suddenly declines, corresponding to a much narrower gap size of 0.003 eV. This behavior is naturally understood in the anisotropic gap size distribution in the charge-density-wave state and indicates that the minority carrier with a much smaller gap size dominates the electrical conduction in the low-temperature range after the thermal excitation of the majority carrier with a larger gap size is suppressed. Interestingly, electrical resistivity shows remarkable magnetic-field (H) dependence below 20 K in $H \parallel [001]$, as seen in Fig. 1(c). In contrast to the fact that the electrical resistivity in $\text{CeTe}_{1.83}\text{Sb}_{0.17}$ below 4 K is 10^8 times higher than the metallic CeTe_2 in previous reports, magnetic properties are basically the same [17], indicating that contribution of RKKY interaction is less important in the magnetic order.

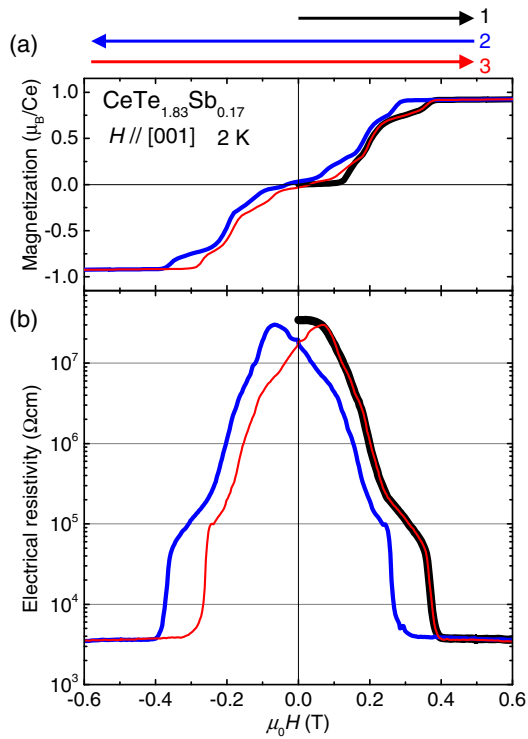


FIG. 2. (a) Magnetization and (b) electrical resistivity of $\text{CeTe}_{1.83}\text{Sb}_{0.17}$ at 2 K in a magnetic field along [001].

Figures 2(a) and 2(b) show the magnetization and electrical resistivity of $\text{CeTe}_{1.83}\text{Sb}_{0.17}$ in $H \parallel [001]$ at 2 K, respectively. After cooling in zero field, magnetization is nearly zero, while electrical resistivity is the highest value. Electrical resistivity starts to decrease above 0.02 T and then steeply drops as the magnetic field increases and reaches 1/9000 of the zero-field value at 0.4 T, where the forced ferromagnetic state is realized. Magnetization shows a multistep increase like the Devil's Staircase, implying the collective reorientation of the in-plane ferromagnetic moments [28]. In the magnetic-field scan process, corresponding hysteresis loops are seen in magnetization and electrical resistivity in the antiferromagnetic state. Such a strong influence on the electrical conduction in quadruple digits by spatially separate magnetic layers is a unique feature for the present low carrier density system. In the forced ferromagnetic state above 0.4 T, electrical resistivity is almost constant up to 7 T.

Next, we focus on the anisotropy of magnetoresistance. Figures 3(a) and 3(b) show the magnetization and electrical resistivity measured in $H \parallel [001]$ and $H \parallel [100]$ at 2 K. In contrast to the drastic reduction in $H \parallel [001]$, only the small change is seen in the electrical resistivity in $H \parallel [100]$ up to 7 T, even though the magnetization closes the saturation. Thus magnetoresistance is highly dependent on the magnetic-field direction and the anisotropy exceeds 7500 at 0.4 T. Such a large anisotropic magnetoresistance is reported here in this low field range that is accessible by commercially used permanent and/or electric magnets. Even in the antiferromagnetic state below 0.4 T, the anisotropy of the magnetoresistance reaches 2 at 0.11 T, 31 at 0.2 T, and 270 at 0.3 T. To reveal the variation of the magnetoresistance as a function of

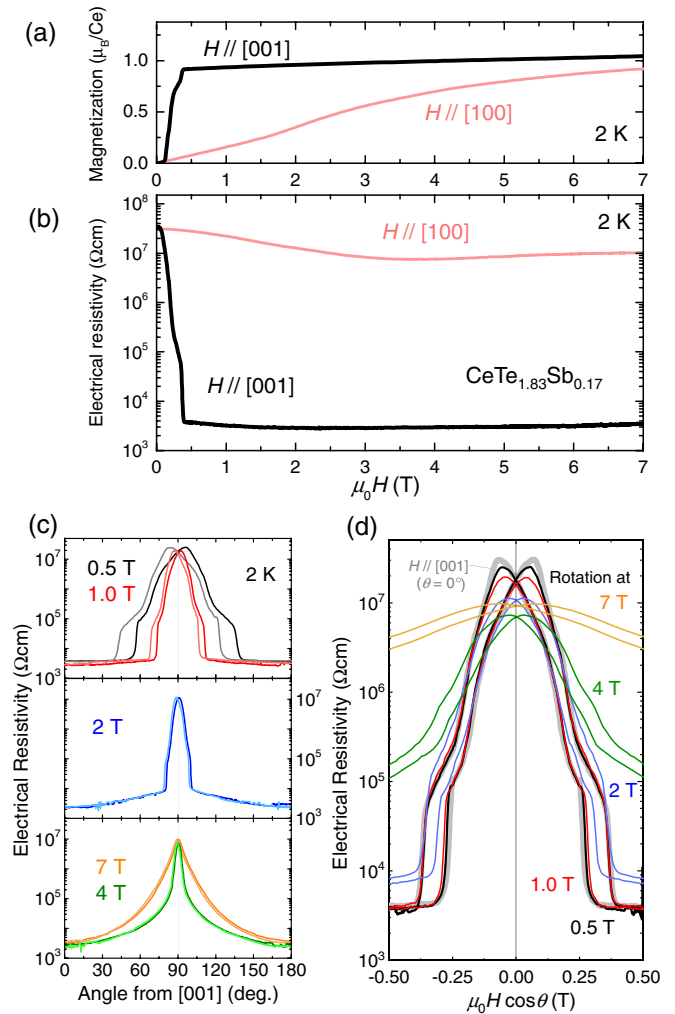


FIG. 3. (a) Magnetization and (b) electrical resistivity of $\text{CeTe}_{1.83}\text{Sb}_{0.17}$ at 2 K in magnetic field along [001] and [100]. (c) Electrical resistivity measured by changing the magnetic-field direction in the (010) plane. (d) Electrical resistivity as a function of the projection field to [001].

the direction of the magnetic field, we measured the electrical resistivity by rotating the magnetic field in the (010) plane. As shown in Fig. 3(c), electrical resistivity shows clear rotation hysteresis at around $H \parallel [100]$ ($\theta = 90^\circ$) and then decreases when the magnetic-field direction is away from [100]. Remarkably, electrical resistivity data obtained in the rotation measurements below 2 T are basically on the same curve as a function of the projection field to [001] direction ($\mu_0 H \cos \theta$) [Fig. 3(d)], revealing that the electrical resistivity is governed by the out-of-plane component of magnetization. Figures 4(a) and 4(b) show magnetic-field dependence of the magnetization and electrical resistivity at various temperatures in $H \parallel [001]$. Below 3 K, electrical resistivity sharply drops in a magnetic field nearly at 0.4 T, corresponding to the steep increase of magnetization from antiferromagnetic to field-induced ferromagnetic state. On the other hand, electrical resistivity decreases smoothly above 3.5 K, corresponding to the gradual increase of the magnetization. Even above the antiferromagnetic transition temperature, electrical resistivity

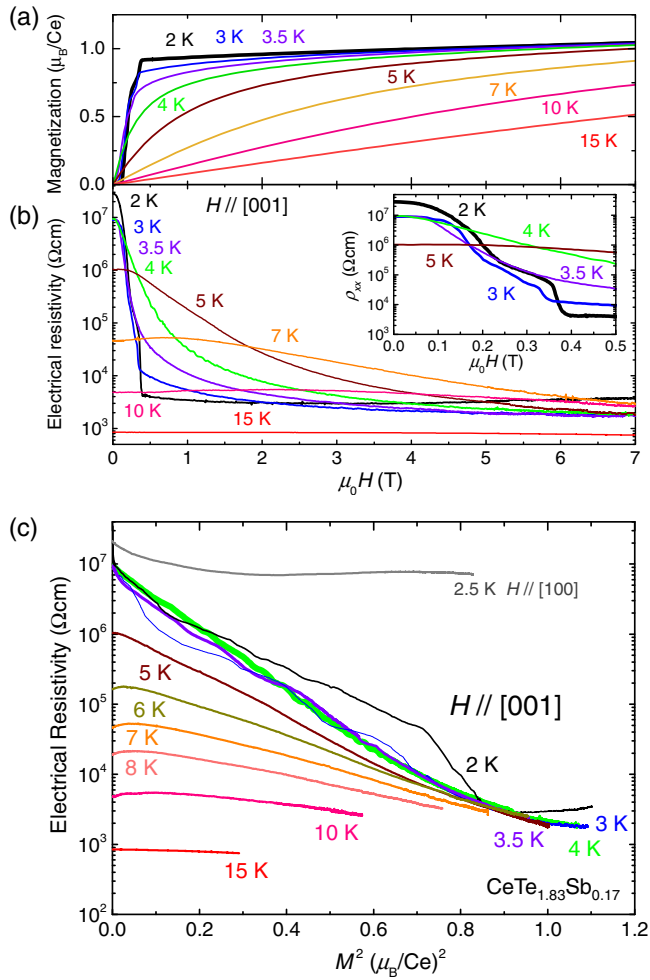


FIG. 4. (a) Magnetization and (b) electrical resistivity of $\text{CeTe}_{1.83}\text{Sb}_{0.17}$ at various temperatures in $H \parallel [001]$. Inset shows the magnified view in the low magnetic-field range. (c) Electrical resistivity as a function of the square of magnetization in (a) and (b). On a logarithmic scale, electrical resistivity decreases rectilinearly and approaches the constant value at the magnetization saturation.

reduces to be 1/5000 at 4 K at 7 T, and the negative magnetoresistance is observed up to 15 K. Variation of the charge-density-wave state in this low temperature range has not been reported and the direct relation with the magnetoresistance is unclear. From these data in Figs. 4(a) and 4(b), we found the relation between electrical resistivity and magnetization in a magnetic field along [001]. As shown in Fig. 4(c), logarithmic electrical resistivity shows almost linear dependence as a function of the square of the uniaxial magnetization ($\ln \rho_{xx} \propto M_{[001]}^2$) in a wide temperature range. This relation is seen only in the out-of-plane component of magnetization. While the slope in the $\ln \rho$ vs $M_{[001]}^2$ becomes larger as temperature decreases, electrical resistivity approaches the constant value when magnetization gets close to the saturation, irrespective of the temperature. Thus we consider the magnetic polaron mechanism for the low-density charge carrier survived in the charge-density-wave state is the plausible origin of the present giant magnetoresistance. The crossover from the localization of charge carrier in the param-

agnetic state to the delocalization in the forced ferromagnetic state is also seen in the peak structure in the temperature dependence of the electrical resistivity in magnetic fields in Fig. 1(c).

Recently, huge anisotropic magnetoresistance in much higher magnetic field was reported in $\text{Nd}_2\text{Ir}_2\text{O}_7$ [29,30], $\text{Mn}_3\text{Si}_2\text{Te}_6$ [31,32], EuMnSb_2 [33], and EuTe_2 [34,35]. In pyrochlore $\text{Nd}_2\text{Ir}_2\text{O}_7$, the $5d$ band crosses the Fermi level only in the specific orientation pattern of the local Nd- $4f$ moments through the exchange interaction, while in the latter compounds, the excitation gap size changes, depending on the spin direction via spin orbit interaction. Thus metal-insulator transition occurs in those materials in low temperature range by changing the magnetic-field direction. Compared with these materials, giant magnetoresistance in $\text{CeTe}_{1.83}\text{Sb}_{0.17}$ occurs in a very high-resistive range in the charge-density-wave state. Nearly four orders of anisotropic magnetoresistance was observed above 0.4 T, originating from the exclusive coupling with the out-of-plane component of magnetization. Since the required magnetic field is very low, the electrical resistivity can be controlled in quadruple digits just by touching or removing or rotating the commercially available permanent magnet (e.g., > 0.4 T in neodymium-based magnet) and/or electronic magnet. Furthermore, by using the soft ferromagnets as a variable magnetic-field source, much lower external magnetic-field control or detection might be possible on the scale of the coercive field of the magnets through the variation of the magnetization. It is of great interest that the Ce compound ($4f^1$) shows such a huge scale of negative magnetoresistance comparable with the Eu-based compounds ($4f^7$), in which the magnetoresistance tends to be very large by the magnetic polaron mechanism owing to the strong exchange coupling between conducting carrier and local $4f$ moment [13,33]. Even after the drastic reduction in $H \parallel [001]$, electrical resistivity in the forced ferromagnetic state in $\text{CeTe}_{1.83}\text{Sb}_{0.17}$ is very high $\approx 1800 \Omega \text{cm}$, which is 10^4 – 10^6 times higher than the typical value in the field-induced metallic state in the other antiferromagnets. Therefore, $\text{CeTe}_{1.83}\text{Sb}_{0.17}$ is the unique system exhibiting the magnetotransport properties in the low carrier density limit. Further investigation for the magnetoresistance in charge-density-wave semiconductors composed of other rare earth ions ($R\text{Te}_2$) might be helpful to understand how the local magnetism affects the carrier mobility and density in the charge-density-wave state and gives rise to the huge anisotropic magnetoresistance.

IV. CONCLUSIONS

In conclusion, we observed the giant anisotropic magnetoresistance reaching nearly four orders of magnitude above 0.4 T in the layered charge-density-wave semiconductor $\text{CeTe}_{1.83}\text{Sb}_{0.17}$. The electrical resistivity is governed by the out-of-plane component of magnetization, while it is quite insensitive to the in-plane component of magnetization. Even after the significant reduction in $H \parallel c$, electrical resistivity in the field-induced state is still unusually high. Those are the unique magnetotransport phenomena in the layered semiconductor with extremely low carrier density.

ACKNOWLEDGMENTS

We thank Y. Narumi and K. Miyake for fruitful discussions. This work was in part supported by JSPS KAKENHI Grants No. JP18H04226, No. JP21K03445, No. JP19H01851, and No. JP21H00147 from the Japan Science Society, and by the Murata Science Foundation, Asahi Glass Foundation,

and at the Center for Spintronics Research Network (CSRN), Graduate School of Engineering Science, Osaka University. This work was carried out at the Center for Advanced High Magnetic Field Science at Osaka University under the Visiting Researcher's Program of the Institute for Solid State Physics, the University of Tokyo.

- [1] J. M. Ziman, *Principles of the Theory of Solids*, 2nd ed. (Cambridge University Press, New York, 1972).
- [2] A. B. Pippard, *Magnetoresistance in Metals* (Cambridge University Press, Cambridge, UK, 1989).
- [3] M. N. Baibich, J. M. Broto, A. Fert, F. Nguyen Van Dau, F. Petroff, P. Etienne, G. Creuzet, A. Friederich, and J. Chazelas, *Phys. Rev. Lett.* **61**, 2472 (1988).
- [4] M. N. Ali, J. Xiong, S. Flynn, J. Tao, Q. D. Gibson, L. M. Schoop, T. Liang, N. Haldolaalachichige, M. Hirschberger, N. P. Ong, and R. J. Cava, *Nature (London)* **514**, 205 (2014).
- [5] C. Shekhar, A. K. Nayak, Y. Sun, M. Schmidt, M. Nicklas, I. Leermakers, U. Zeitler, Y. Skourski, J. Wosnitza, Z. Liu, Y. Chen, W. Schnelle, H. Borrmann, Y. Grin, C. Felser, and B. Yan, *Nat. Phys.* **11**, 645 (2015).
- [6] P. B. Alers and R. T. Webber, *Phys. Rev.* **91**, 1060 (1953).
- [7] K. Yokoi, H. Murakawa, M. Komada, T. Kida, M. Hagiwara, H. Sakai, and N. Hanasaki, *Phys. Rev. Materials* **2**, 024203 (2018).
- [8] A. Urushibara, Y. Moritomo, T. Arima, A. Asamitsu, G. Kido, and Y. Tokura, *Phys. Rev. B* **51**, 14103 (1995).
- [9] H. Kuwahara, Y. Tomioka, A. Asamitsu, Y. Moritomo, and Y. Tokura, *Science* **270**, 961 (1995).
- [10] N. Hanasaki, H. Tajima, M. Matsuda, T. Naito, and T. Inabe, *Phys. Rev. B* **62**, 5839 (2000).
- [11] N. Hanasaki, M. Matsuda, H. Tajima, E. Ohmichi, T. Osada, T. Naito, and T. Inaba, *J. Phys. Soc. Jpn.* **75**, 033703 (2006).
- [12] H. Murakawa, A. Kanda, M. Ikeda, M. Matsuda, and N. Hanasaki, *Phys. Rev. B* **92**, 054429 (2015).
- [13] P. Rosa, Y. Xu, M. Rahn, J. Souza, S. Kushwaha, L. Veiga, A. Bombardi, S. Thomas, M. Janoschek, E. Bauer, M. Chan, Z. Wang, J. Thompson, N. Harrison, P. Pagliuso, A. Bernevig, and F. Ronning, *npj Quantum Mater.* **5**, 52 (2020).
- [14] A. P. Ramirez, *J. Phys.: Condens. Matter* **9**, 8171 (1997).
- [15] E. Dagotto, T. Hotta, and A. Moreo, *Phys. Rep.* **344**, 1 (2001).
- [16] Y. Tokura, *Rep. Prog. Phys.* **69**, 797 (2006).
- [17] M. H. Jung, B. H. Min, Y. S. Kwon, I. Oguro, F. Iga, T. Fujita, T. Ekino, T. Kasuya, and T. Takabatake, *J. Phys. Soc. Jpn.* **69**, 937 (2000).
- [18] M. H. Jung, K. Umeo, T. Fujita, and T. Takabatake, *Phys. Rev. B* **62**, 11609 (2000).
- [19] T. Kasuya, M. H. Jung, and T. Takabatake, *J. Magn. Magn. Mater.* **220**, 235 (2000).
- [20] B. H. Min, E. D. Moon, H. J. Im, S. O. Hong, Y. S. Kwon, D. L. Kim, and H. C. Ri, *Phys. B: Condens. Matter* **312-313**, 205 (2002).
- [21] K. Y. Shin, V. Brouet, N. Ru, Z. X. Shen, and I. R. Fisher, *Phys. Rev. B* **72**, 085132 (2005).
- [22] J. S. Kang, D. H. Kim, H. J. Lee, J. Hwang, H. K. Lee, H. D. Kim, B. H. Min, K. E. Lee, Y. S. Kwon, J. W. Kim, K. Kim, B. H. Kim, and B. I. Min, *Phys. Rev. B* **85**, 085104 (2012).
- [23] E. Lee, D. H. Kim, J. D. Denlinger, J. Kim, K. Kim, B. I. Min, B. H. Min, Y. S. Kwon, and J. S. Kang, *Phys. Rev. B* **91**, 125137 (2015).
- [24] J. G. Park, I. P. Swainson, W. J. L. Buyers, M. H. Jung, and Y. S. Kwon, *Physica B* **241-243**, 684 (1998).
- [25] J. G. Park, Y. S. Kwon, W. Kockelmann, M. J. Bull, I. P. Swainson, K. A. McEwen, and W. J. L. Buyers, *Phys. B: Condens. Matter* **281-282**, 451 (2000).
- [26] K. E. Lee, S. Kim, B. H. Min, J. S. Rhyee, J. N. Kim, J. H. Shim, and Y. S. Kwon, *Appl. Phys. Lett.* **101**, 143901 (2012).
- [27] M. H. Jung, Y. S. Kwon, and T. Suzuki, *Phys. B: Condens. Matter* **240**, 83 (1997).
- [28] R. Singha, T. H. Salters, S. M. L. Teicher, S. M. Lei, J. F. Khoury, N. P. Ong, and L. M. Schoop, *Adv. Mater.* **33**, 2103476 (2021).
- [29] K. Ueda, J. Fujioka, B.-J. Yang, J. Shiogai, A. Tsukazaki, S. Nakamura, S. Awaji, N. Nagaosa, and Y. Tokura, *Phys. Rev. Lett.* **115**, 056402 (2015).
- [30] Z. Tian, Y. Kohama, T. Tomita, H. Ishizuka, H. T. Hsieh, J. J. Ishikawa, K. Kindo, L. Balents, and S. Nakatsuji, *Nat. Phys.* **12**, 134 (2016).
- [31] Y. Ni, H. Zhao, Y. Zhang, B. Hu, I. Kimchi, and G. Cao, *Phys. Rev. B* **103**, L161105 (2021).
- [32] J. Seo, C. De, H. Ha, J. E. Lee, S. Park, J. Park, Y. Skourski, E. Sang, C. B. Kim, G. Y. Cho, H. W. Yeom, S. W. Cheong, J. H. Kim, B. J. Yang, K. Kim, and J. S. Kim, *Nature (London)* **599**, 576 (2021).
- [33] Z. L. Sun, A. F. Wang, H. M. Mu, H. H. Wang, Z. F. Wang, T. Wu, Z. Y. Wang, X. Y. Zhou, and X. H. Chen, *npj Quantum Mater.* **6**, 94 (2021).
- [34] J. Yin, C. Wu, L. Li, J. Yu, H. Sun, B. Shen, B. A. Frandsen, D.-X. Yao, and M. Wang, *Phys. Rev. Materials* **4**, 013405 (2020).
- [35] H. Yang, Q. Liu, Z. Liao, L. Si, P. Jiang, X. Liu, Y. Guo, J. Yin, M. Wang, Z. Sheng, Y. Zhao, Z. Wang, Z. Zhong, and R. W. Li, *Phys. Rev. B* **104**, 214419 (2021).